THE DEEP IMPACT CRATER AS SEEN FROM THE STARDUST-NEXT MISSION. P. H. Schultz[1], B. Hermalyn[1], and Joe Veverka[2], [1]Brown University Geological Sciences, 324 Brook St., Box 1846, Providence, RI 02912; [2]Cornell University, Ithaca, NY 14853, peter_schultz@brown.edu.

Introduction: The *Deep Impact* (*DI*) mission guided a ~370kg probe into the nucleus of comet 9P/Tempel-1. The cratering experiment ejected material from depth, allowing spectral observations of pristine, subsurface ices and dust from a cometary nucleus for the first time [1]. Measurements of the distinctive evolution of the ejecta from the cratering process itself [2] and the gravity-controlled advance of the ejecta curtain (e.g., [1, 3]) provided the first constraints on the bulk density of the nucleus. Fine ballistic dust ballistically rising above the impact site, however, obscured the crater from view throughout the entire approach. The return to 9P/Tempel-1 by the *Stardust-NExT* (*SdN*) mission allowed assessment of both the changes to the nucleus and the appearance of the crater formed by the *DI*-probe 5.5 years after the first encounter. Because of uncertainties in the rotation rate of the nucleus, observation of the crater by *SdN* was not raised to the level of a primary objective.

DI Crater and Its Surroundings: At closest approach to the nucleus of 9P Tempel-1, the *SdN* imaging system achieved a resolution of ~11m/pxl corresponding to a working resolution 2.2 pixels (in order to resolve features). Figure 1 allows direct comparison between the pre-impact images from the camera on board the ITS probe itself and *SdN* images. The ITS approach images have much higher spatial resolution just before impact; nevertheless, small features close to the resolution limit can be readily identified in *SdN* images. Based on multiple approaches, the impact point was just to the right of a small, dark mound (cross in Fig. 1a), which now appears very muted. This loss of expression is not attributed to differences in resolution since comparable-scale features can be identified elsewhere in the two images. Successive images (with changing phase angles) provide much greater confidence in the identification of a subtle (but obvious) 50m-diameter dimple at the location of impact (Fig. 1b). Images under different viewing angles (as well as stereo pairs) also reveal a subtle arcuate outer rim about 180m in diameter (Fig. 2) that overlaps the region with the missing mound labeled.

There are four explanations why the *SdN* images did not reveal a large, deep crater. First, the crater was small due to unique properties of the surface of the nucleus (e.g., [4]). Second, the crater collapsed soon after formation due to the deep penetration by the DI probe. Third, localized mass wasting (e.g., localized venting and wall collapse) destroyed the final crater after 5.5 years. Fourth, the crater is a nested crater, i.e., a small central crater surrounded by a broad but shallow-rimmed excavated zone. These alternatives are considered in more detail.

Constraints on Initial Crater Size: The closest approach to the nucleus by the DI flyby provided evidence of a large crater: the ballistic ejecta curtain filled half of the field of view and obscured underlying topography for more than 700 seconds after impact. A stereo view reveals two shadows emerging from the impact site from a high-angle ejecta plume: one cast on the interior of the ejecta curtain, the other revealed below on the surface as the curtain becomes transparent farther above. Comparison between surface features before and after the impact reveals that the ejecta are optically thick at least 0.5km above the surface (viewed face on) but at a much greater distance from the surface (viewed down, along the curtain in the foreground). The amount of obscuration 6-10 crater diameters above the surface is inconsistent for a small crater (only 50m in diameter).

Co-location of features in pre- and post-impact images constrains the impact point within 50 m. Ballistic ejecta rays projected back to the surface converge on an elliptical footprint at the surface but significantly downrange from the impact point. A high-angle plume casts a shadow on the interior of the ejecta curtain and hides the actual contact between curtain and the surface. The elliptical footprint actually corresponds to the base of the ejecta curtain, rather than the final crater. About 700s after impact, the ejecta curtain had grown to a diameter of ~370 m (± 50m).

The downrange offset of the ejecta-curtain base reflects an expected evolution of the ejecta curtain in a loose, porous particulate target. For vertical impacts, the ejecta-curtain base (or slice through the curtain, e.g., [5]) expands in concentric circles centered at the impact point. For oblique impacts, however, the base of the ejecta curtain appears pinned to near the impact point [2]. In under-dense (highly porous and compressible) targets, the impact point is just inside the uprange wall, rather than the crater center. Similarly, the shadow from the high-angle plume for the DI impact extends back to a point considerably downrange from the impact point. This migration reflects the downrange velocity component of individual particles within the late-stage high-angle ballistic plume, a motion also observed in laboratory experiments using highly porous and compressible targets.

Two additional observations from the DI encounter indicate an excavation crater significantly larger than the relict 50m-diameter pit. First, a small mound near the impact point (Fig. 1b) altered the pattern of ballistic ejecta uprange as seen from the DI flyby. Second, an

extension from the scarp downrange from the impact point (also Fig. 1b) created a gap in the ejecta curtain. These two observations constrain the excavation crater diameter to about 200m along the trajectory.

A crater 50m in diameter would have ejected only a fraction of the observed mass ejected by the DI collision, estimated to be about 8×10^6 kg of dust and ice [7,8]]Such observations refer only to materials that left the gravity field completely, not the fraction that returned to the surface. Consequently, the total amount of material excavated by the impact actually represents a factor 3 to 10 greater than estimates from telescopic observations. Hence, the observed amount of dust and ice is consistent with a crater nearly 150-200m in diameter

***Nested Crater*:** The faint outer rim (180m in diameter) identified in different look directions and stereo image pairs resembles nested craters found on the Moon (Fig. 3). On the Moon and in laboratory experiments, nested craters are produced by impacts into a thin, loose layer of particulates covering a competent substrate [6]. In this case, the classical ejecta curtain still forms, but the thickness of the curtain is significantly reduced due to the arrested flow field. The muted appearance of topography and numerous layers inferred from close-up images by the ITS camera during approach indicate that a similar layering occurs at the DI impact site. Even small contrasts in target strength limits downward displacement in the low-speed flow field due to the very weak gravity and weak shock conditions at large distances from the impact (porous target). Rather than a solid competent subsurface (as on the Moon), the substrate at the DI impact site is probably more strongly bonded than the loose surface layer yet still strong enough to produce a nested crater

Conclusions: Based on the observations from the *SdN* and the evolution of the DI excavation sequence, we conclude that two interpretations are the most reasonable: a large (~200m in diameter) transient crater that collapsed, or a nested crater with a small inner pit (~50m in diameter) surrounded by a shallow excavation crater (~180m in diameter). Both alternatives can be directly related to surface features in Stardust-NExT images and are consistent with published estimates for the amount of ejecta excavated by the DI collision.

References: [1] A'Hearn, M.F. *et al.* (2005), *Science* 310, 258-264; [2] Schultz, P. H., *et al.* (2007), *Icarus* 190, 295-333; [3] Richardson, J. E., *et al.* (2007), *Icarus*, 190, 357 – 390; [4] Housen, K.R. *et al.* (1999), *Nature* 402, 155-157; [5] Anderson, J. L. B. *et al.* (2003), *J. Geophys. Res.*108, No. E8, 5094, 10.1029/2003JE002075; [6] Quaide, W.L., and Oberbeck, V.R. (1968), *J. Geophys. Res.*, 73, 5247-5270; [7] Keller *et al*. (2005), Science 310, 281–283; [8] Lisse *et al*. (2006), *Science* 313, 635-640.

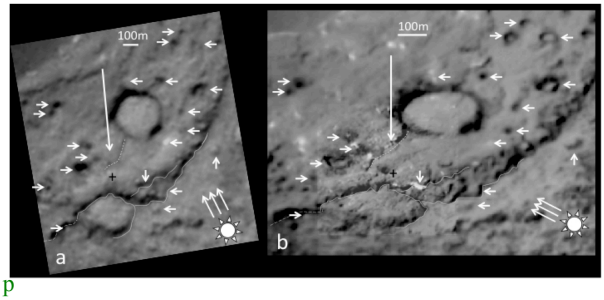

p

Figure 1: Comparison of common features identified in *Stardust-NExT* image at left and the composite ITS image from Deep Impact at right. In order to enable comparisons, the vertical scale is preserved in deference to the horizontal scale. This is necessary due to extreme foreshortening created during approach by the DI probe (right). Small cross (black) indicates the best-fit location for the DI impact. The small mound adjacent to the impact site in the pre-impact image (right) appears degraded in the *Stardust-NExT* image (left).

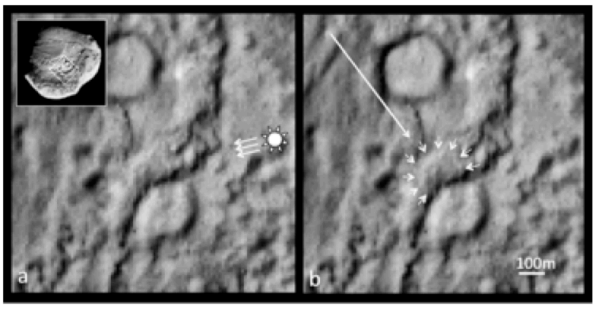

Figure 2: Close views of the impact site (see inset for context) in *Stardust-NExT* image frame with illumination from the right. Long arrow indicates the approximate trajectory of the DI probe. A small depression (~50 m in diameter) occurs at the expected site of the DI impact. Small arrows identify a subtle but identifiable ring about 180m in diameter.

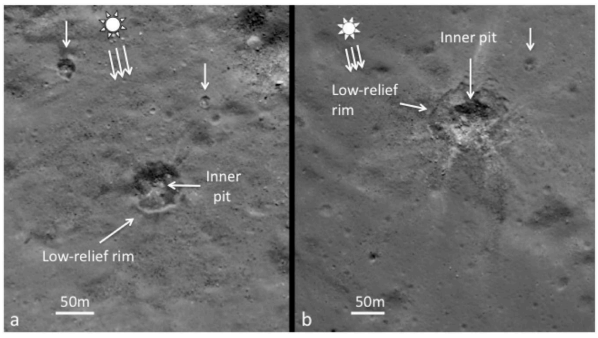

Figure 3: Examples of nested craters on the impact melt downrange of King crater on the Moon. Nested craters form by impacts into a layered target. The inner pit results from penetration through a thin regolith into a competent substrate and reflects strength scaling. The outer rim forms by excavation of the overlying regolith, controlled by gravity scaling.